IEEE/CSC & ESAS European Superconductivity News Forum (ESNF), No. 15, January 2011
The published version of this manuscript appeared in *IEEE Transactions on Applied Superconductivity* **21**, Issue 3, 354 - 357 (2011)

Voltage Biased SQUID Bootstrap Circuit: Circuit Model and Numerical Simulation

Yongliang Wang, Xiaoming Xie, Hui Dong, Guofeng Zhang, Huiwu Wang, Yi Zhang, Michael Mück, Hans-Joachim Krause, Alex. I. Braginski, *IEEE Life Fellow*, Andreas Offenhäusser, and Mianheng Jiang

***Abstract*—The SQUID Bootstrap Circuit (SBC) for direct-coupled readout of SQUID signals in voltage bias mode was recently demonstrated. In addition to the conventional dc SQUID, the SBC incorporates a shunt resistor R_s, and two coils coupled to the SQUID via mutual inductances M_1 and M_2. In this paper, basic equations of SBC are formulated based on its equivalent circuit model. The expression of equivalent flux noise from the preamplifier is also given. The effect of the three adjustable parameters (M_1, M_2 and R_s) on the characteristics of SBC and the preamplifier noise suppression are numerically simulated. The SBC combines current and voltage feedbacks in one circuit, allowing for an effective suppression of the preamplifier voltage noise through increased flux-current transfer coefficient and dynamic resistance. In contrast to other direct-coupled schemes, it offers not only a good noise performance, but also tolerance to a wide range of adjustable parameters.**

***Index Terms*—Noise Suppression, Numerical Simulation, SQUID Bootstrap Circuit, SQUID Direct Readout.**

I. INTRODUCTION

The extremely low intrinsic noise of Superconducting QUantum Interference Device (SQUID) is usually dominated by the room-temperature preamplifier noise. Some help is provided by the standard flux modulation scheme [1], in which a transformer is used to step up the signal voltage and to improve the impedance matching between SQUID and the preamplifier. However, in multichannel SQUID applications, simplification of the readout electronics is desired.

Alternative, simpler readout schemes [2]–[7] include the current-biased additional positive feedback (APF) [5] and the voltage-biased noise cancellation (NC) [7]. A generalized analysis of such direct-coupled readout schemes was recently offered by Drung [8]. The recently reported SQUID Bootstrap Circuit (SBC) [9] is another variant of these.

Here, we propose the equivalent circuit model and the basic equations of SBC to improve understanding of its performance. Numerical simulations based on this model render properly the current-flux and current-voltage characteristics, and also the preamplifier noise suppression. Further simulations should facilitate optimization of SBC parameters.

II. EQUIVALENT CIRCUIT AND BASIC EQUATIONS

The SBC works under a constant bias voltage V_b and its schematic diagram is shown in Fig. 1 (a). Its two key features are the current feedback via the mutual inductance M_1 to increase the current flux transfer coefficient of SBC ($\partial i_{SBC}/\partial \Phi_e$), and the voltage feedback via M_2 to enhance the dynamic resistance of SBC, R_d^{SBC}. Preliminary noise measurements using the SBC readout demonstrated intrinsic SQUID noise performance, and parameter adjustment tolerance wider than for either APF or NC [9], [10].

We view the SBC in Fig. 1 (a) as a two-terminal device, a SQUID shunted by the resistor R_s, where the impedances of inductances L_1 and L_2 in SBC can be neglected in the low frequency limit. Two additional fluxes are fed back to SQUID via M_1 and M_2.

The SBC equivalent circuit is presented in Fig. 1 (b). At the bias voltage V_b, the total current flowing through the SBC, i_{SBC}, is the sum of two parts, i_1 and i_2, where i_1 is the current flowing through the SQUID. It can be defined as a function f of V_b and of the total flux applied to the SQUID Φ_T:

$$i_1 = f(V_b, \Phi_T)\,, \tag{1}$$

in which the total applied flux Φ_T is a sum of the external signal flux Φ_e and of both feedback fluxes: $\Phi_T = \Phi_e + M_1 \cdot i_1 + M_2 \cdot i_2$. In contrast, the current through R_s always keeps the relation: $i_2 = V_b/R_s$. The current i_{SBC} is thus also a function of V_b and Φ_e, as defined in (2).

Manuscript received 3 August 2010. This work was supported by several funding sources: the bilateral cooperation on education and research, the International Bureau of the German BMBF at DLR, Grant No. CHW09/009; funding from National 863 Project (contract number: 2008AA02z308) and Shanghai Committee of Science and Technology (contract number: 08JC1421800); funding from Chinese Academy of Sciences for international cooperation (contract number: GJHZ1104).

Y. Wang, H. Wang, X. Xie and M. Jiang are with State Key Laboratory of Functional Materials for Informatics, Shanghai Institute of Microsystem and Information Technology, Chinese Academy of Sciences, Shanghai 200050, P. R. China (phone: ++86-21-52419909; fax: ++86-21-52419909; e-mail: xmxie@mail.sim.ac.cn).

H. Dong and G. Zhang are visitors from Shanghai Institute of Microsystem and Information Technology, Chinese Academy of Sciences, Shanghai 200050, P. R. China, and Graduate University of the Chinese Academy of Sciences, Beijing 100049, P. R. China, to Forschungszentrum Jülich, D-52425, Jülich, Germany.

Y. Zhang, H. -J. Krause, A. I. Braginski and A. Offenhäusser are with Institute of Bio- and Nanosystems (IBN-2) Forschungszentrum Jülich, D-52425, Jülich, Germany (e-mail: y.zhang@fz-juelich.de).

M. Mück is with Institut für Angewandte Physik, Justus-Liebig-Universität Gießen, D-35392 Gießen, Germany.

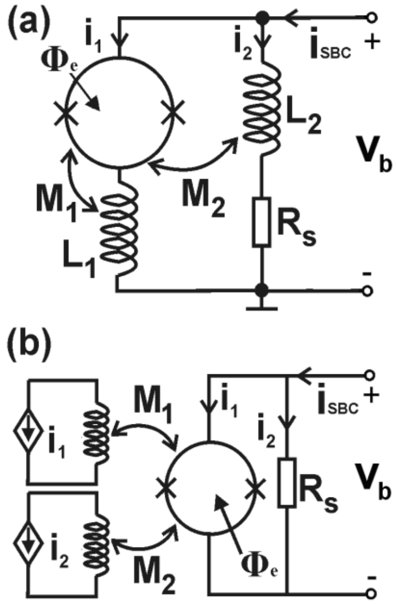

Fig. 1. (a) Illustration of SBC based on voltage bias mode, a two-terminal device with two parallel branches. Branch 1 consists of the SQUID and a coil L_1, and branch 2 consists of a coil L_2 and a shunt resistor R_s. (b) The equivalent circuit model of SBC in the low frequency limit ωL_i (i = 1, 2) → 0. The SQUID is shunted by the resistor R_s, and coupled via the mutual inductances, M_1 and M_2 to two separate closed feedback circuits, each consisting of a current source and a coil.

$$\begin{aligned} i_{SBC} &= i_1 + i_2 \\ &= f\left(V_b, \Phi_e + M_1\cdot\left(i_{SBC} - \frac{V_b}{R_s}\right) + M_2\cdot\frac{V_b}{R_s}\right) + \frac{V_b}{R_s} \end{aligned} \tag{2}$$

The dynamic resistance R_d and the flux-to-current transfer coefficient ($\partial i_1/\partial\Phi_T$) of the conventional SQUID in SBC can be defined from the expression (1):

$$\begin{aligned} \frac{1}{R_d} &= \frac{\partial i_1}{\partial V_b} = \frac{\partial f(V_b,\Phi_T)}{\partial V_b} \\ \frac{\partial i_1}{\partial \Phi_T} &= \frac{\partial f(V_b,\Phi_T)}{\partial \Phi_T} \end{aligned} \tag{3}$$

With (2) and (3), the partial differential equation relating i_{SBC}, V_b, and Φ_e is:

$$\begin{aligned} di_{SBC} &= \left(\frac{1}{R_d} + \frac{\partial i_1}{\partial \Phi_T}\cdot\frac{(M_2 - M_1)}{R_s} + \frac{1}{R_s}\right)\cdot dV_b \\ &\quad + \frac{\partial i_1}{\partial \Phi_T}\cdot M_1\cdot di_{SBC} + \frac{\partial i_1}{\partial \Phi_T}\cdot d\Phi_e \end{aligned} \tag{4}$$

As V_b is nominally constant in the voltage bias mode, the flux-to-current transfer coefficient of the SBC is:

$$\frac{\partial i_{SBC}}{\partial \Phi_e} = \frac{di_{SBC}}{d\Phi_e} = \frac{1}{1 - \frac{\partial i_1}{\partial \Phi_T}\cdot M_1}\cdot\frac{\partial i_1}{\partial \Phi_T} \tag{5}$$

At constant Φ, the dynamic resistance R_d^{SBC} of SBC can be expressed as:

$$R_d^{SBC} = \frac{dV_b}{di_{SBC}} = \frac{R_s\cdot R_d\cdot\left(1 - \frac{\partial i_1}{\partial \Phi_T}\cdot M_1\right)}{R_s + R_d\cdot\left(1 + \frac{\partial i_1}{\partial \Phi_T}\cdot(M_2 - M_1)\right)} \tag{6}$$

The product of the two equations above gives the flux-to-voltage transfer coefficient of SBC, $(\partial V/\partial\Phi)^{SBC}$.

Normally, the noise current (I_n) caused by the voltage noise (V_n) of the preamplifier is the dominant noise source in SBC. Therefore, the equivalent flux noise of the SBC contributed by the preamplifier can be written as:

$$\Phi_n = \frac{I_n}{\frac{\partial i_{SBC}}{\partial \Phi_e}} = \frac{V_n}{R_d^{SBC}\cdot\frac{\partial i_{SBC}}{\partial \Phi_e}} \tag{7}$$

In order to simplify (5)–(7), we introduce two dimensionless parameters $\alpha = R_s/R_d$ and $\beta = M\cdot(\partial i_1/\partial\Phi_T)$. The ratio α is the preamplifier noise suppression factor when $R_s = M_2\cdot(\partial V_b/\partial\Phi_T)$ [7]. The parameter β is a ratio of the geometric mutual inductance and the initial equivalent dynamic inductance of the SQUID in SBC. For L_1 and L_2, $\beta_1 = M_1\cdot(\partial i_1/\partial\Phi_T)$ and $\beta_2 = -M_2\cdot(\partial i_1/\partial\Phi_T)$, respectively. The minus sign indicates opposite winding directions of L_1 and L_2.

Consequently, (5)–(7) can be rewritten as follows in terms of α and β:

$$\frac{\partial i_{SBC}}{\partial \Phi_e} = \left(\frac{\partial i_1}{\partial \Phi_T}\right)\cdot\frac{1}{1-\beta_1} \tag{8}$$

$$R_d^{SBC} = R_d\cdot\frac{\alpha\cdot(1-\beta_1)}{\alpha + 1 - \beta_1 - \beta_2} \tag{9}$$

$$\Phi_n = \Phi_{n0}\cdot\frac{\alpha + 1 - \beta_1 - \beta_2}{\alpha} \tag{10}$$

In (10), $\Phi_{n0} = (V_n/R_d)/(\partial i_1/\partial\Phi_T) = V_n/(\partial V_b/\partial\Phi_T)$ is the equivalent flux noise contribution of a preamplifier to a bare SQUID without SBC.

The simplified (8)–(10) show how in the SBC the bare SQUID characteristics are modified by α, β_1 and β_2. The resulting SBC characteristics are numerically simulated below.

III. Numerical Simulations

For the SQUID with overdamped junctions, the relation between the voltage across the SQUID V_b, the total current flowing through it i_1, and the total flux coupled to SQUID, Φ_T, can be described by the well-known expressions:

$$V_b = R_0\sqrt{i_1^2 - I_C^2} \quad (i_1 \ge I_C); \quad V_b = 0 \quad (i_1 < I_C) \tag{11}$$

$$I_C = \Delta I_{C0}\sin(2\pi\Phi_T/\Phi_0) + I_{C0} \tag{12}$$

Here, R_0 is the shunt resistance of two SQUID junctions. I_C is the critical current of the SQUID modulated by the total flux Φ_T. I_{C0} is the average critical current and ΔI_{C0} is the modulation range of critical current by total flux.

In SBC, the total flux Φ_T determining I_C includes the feedback flux caused by i_2 ($i_2 = V_b/R_s$), while I_C is also related to V_b. Therefore, the value of i_1 can only be simulated numerically. The simulation diagram of SBC is shown in Fig. 2. Here, the bias voltage V_b and external signal flux Φ_e are two input parameters and i_{SBC} is the output parameter. When the values of V_b and Φ_e are set, the iterative loop seeks the numerical solution of i_1 by integration of the difference Δv between V_b and the voltage calculated from (11). When $\Delta v \rightarrow 0$, the stable i_1 is attained. Of course, i_{SBC} is the sum of i_1 and i_2.

Equation (11) does not include the junction capacitances and the Nyquist noise in R_0. Therefore, any frequency and temperature effects possibly modifying the shape of the current-voltage curve are neglected.

In the next section we show the simulated normalized current-flux and current-voltage characteristics of the SBC, and also the dependence of the dynamic resistance and flux noise suppression ratio on the flux Φ_e/Φ_0 at the working point.

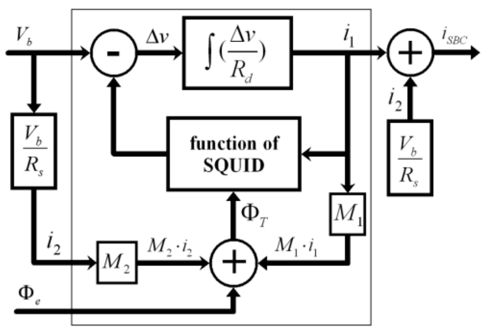

Fig. 2. The numerical simulation diagram

IV. Simulations Results

A. Current-Flux Characteristics

According to (8), the flux-current transfer coefficient $\partial i_{SBC}/\partial \Phi_e$ is determined by the parameter β_1 alone. At constant V_b, i_2 generates only a dc flux coupled into the SQUID. Fig. 3 shows the simulated current-flux characteristics for β_1 increasing in steps from 0 to 2. With increasing β_1 the curves become more and more asymmetrical. The transfer coefficient increases at the steep slope whereas it decreases at the gradual slope. However, the current swing remains constant until β_1 reaches unity, the critical condition of branch 1 in Fig. 1 (a) [9]. With β_1 exceeding unity, the characteristic becomes hysteretic, and the current swing is reduced. The value of β_1 describes the current feedback strength.

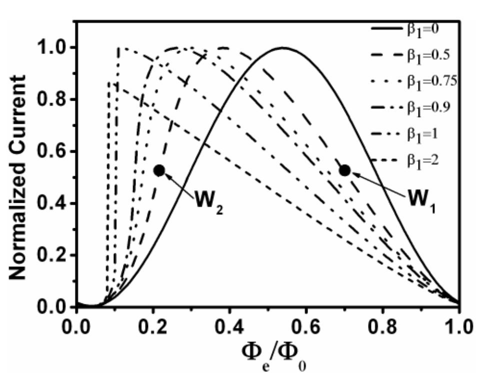

Fig. 3. Simulated current-flux characteristics at different β_1 values. Here, we define W_1 and W_2 as the working points at $\Phi_e = (2n+1)\Phi_0/4$ on two different slopes. Usually W_2 is set at the point of maximum $\partial i_{SBC}/\partial \Phi_e$ on the steep slope of the characteristic.

B. Current-Voltage Characteristics

Calculating the current-voltage characteristic is important, because its slope defines the dynamic resistance R_d^{SBC} at different working points.

For reference, we first show in Fig. 4 two experimental current-voltage curves of the SBC recorded at $\Phi_e = n\Phi_0$ and $\Phi_e = (n+1/2)\Phi_0$. These curves contain two parts: linear (a) and nonlinear (b). On (a), the current through the SQUID should be less than the critical current I_C. The resistance (finite slope) exhibited in the (a) range is caused by the sum of contact resistance and line resistance. We included it in our simulation. The nonlinear resistive range within the dashed rectangle where $i_1 > I_C$ is simulated and plotted in Fig. 5.

The simulated current-voltage characteristics are influenced by different values of the parameters α, β_1 and β_2. For simplicity, Fig. 5 compares two typical cases, one with $\beta_1 = 0.75$ and the other with $\beta_1 = 0$, which is the case of noise cancellation (NC) [7]. For both cases, the comparison is further broken down into two sub-cases: in Fig. 5 (a) and Fig. 5 (c) β_2 is fixed while α is varied; in Fig. 5 (b) and Fig. 5 (d) α is fixed and β_2 varied.

Fig. 5 (a) and (c) show that raising α increases the slope, *i.e.*, decreases the dynamic resistance R_d^{SBC}, while Fig. 5 (b) and Fig. 5 (d) show that R_d^{SBC} increases with β_2.

By comparing the two cases with different β_1, the slope variation at $\beta_1 = 0.75$ is distinctly larger than at $\beta_1 = 0$, when changing either α or β_2.

C. Noise Suppression Dependence on the Working Point

Equations (8), (9) and the simulation results of Fig. 3 and 5 show that the flux-to-current transfer coefficient $\partial i_{SBC}/\partial \Phi_e$, and the dynamic resistance R_d^{SBC} can be *independently* increased compared with those of the bare SQUID. As indicated by (7), the equivalent flux noise from the preamplifier Φ_n can thus be reduced by increasing the product of $\partial i_{SBC}/\partial \Phi_e$ and R_d^{SBC}. This

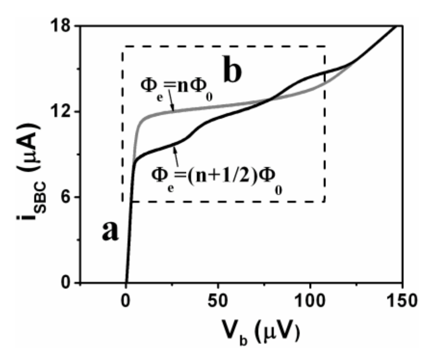

Fig. 4. The experimentally recorded current-voltage curves of a voltage-biased SBC at $\Phi_e = n\Phi_0$ and $\Phi_e = (n+1/2)\Phi_0$.

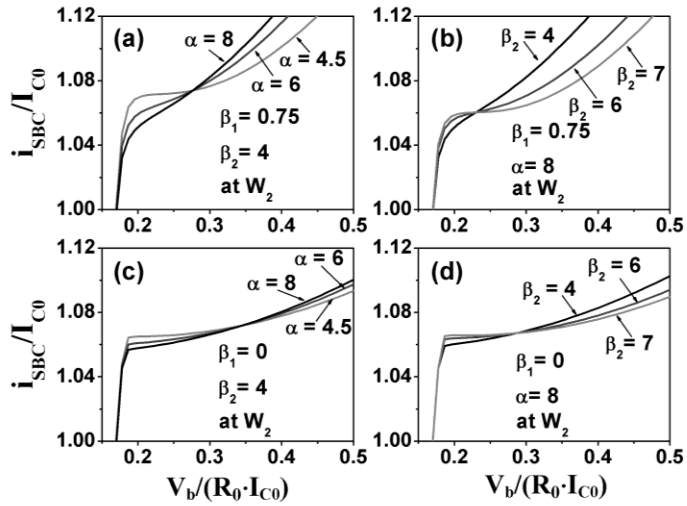

Fig. 5. Simulated current-voltage characteristics of SBC with different combinations of α and β_2 at $\beta_1 = 0$ and 0.75.

allows for a good flexibility in the parameter choice and wide margins for their adjustment.

Both $\partial i_{SBC}/\partial\Phi_e$ and R_d^{SBC} are working-point-dependent as demonstrated by the typical example in Fig. 6 with $\beta_1 = 0.75$, $\beta_2 = 4$, $\alpha = 4$. Fig. 6 (a) shows the normalized asymmetric current-flux characteristic. Fig. 6 (b) shows plots of $\partial i_{SBC}/\partial\Phi_e$ and R_d^{SBC} as functions of Φ_e/Φ_0 chosen as the working point within one flux period Φ_0. Finally, Fig. 6 (c) gives the plot of the preamplifier noise suppression ratio *versus* Φ_e/Φ_0. The vertical dashed lines indicate the working point window in which the noise from the preamplifier can be suppressed. It can be seen that at the optimum working point W_2, $\partial i_{SBC}/\partial\Phi_e$ and R_d^{SBC} increased by a factor of 4 each, giving the total preamplifier noise suppression by a factor of ~16, which should bring it well below the SQUID intrinsic noise level.

As the noise performance involves interaction of three parameters in a nonlinear form, the noise optimization by experiment would be time-consuming. However, this can be easily done by simulation. Therefore, the simulation can be considered as a powerful tool for SBC optimization.

V. Conclusions

In conclusion, we formulated the simplified circuit model of the SQUID Bootstrap Circuit (SBC). The SQUID is shunted by the resistor R_s, and coupled via the mutual inductances, M_1 and M_2 to two separate closed feedback circuits, each consisting of a current source and a coil. The model is described by three equations giving $\partial i_{SBC}/\partial\Phi_e$, R_d^{SBC} and Φ_n. Three dimensionless parameters α, β_1 and β_2 were introduced to simplify the analysis and simulation. Numerical simulations of the current-flux and current-voltage characteristics, and of the preamplifier noise suppression, were performed for different parameters α and β. We showed that the SBC provides a good flexibility in parameter choice and wide margins for their adjustment. The

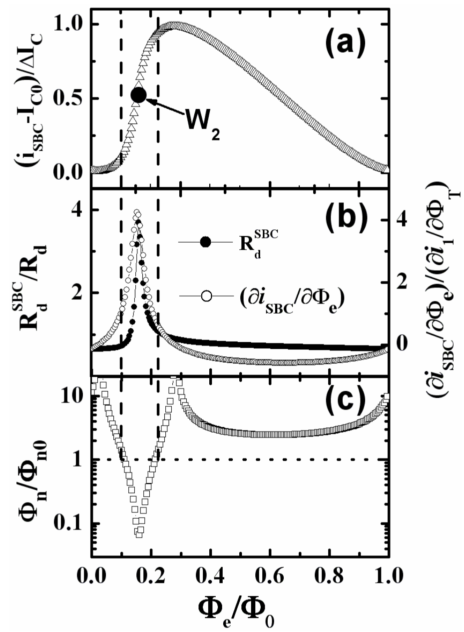

Fig. 6. *I*-Φ characteristics of SBC (a), values of the R_d^{SBC} and $\partial i_{SBC}/\partial\Phi_e$ (b), and the flux noise suppression ratio of SBC Φ_n/Φ_{n0} (c), as a function of external flux in one Φ_0 period.

preamplifier noise suppression can be easily simulated at different sets of parameters. Simulations will thus be useful for the future SBC optimization.

References

[1] R. L. Forgacs, and A. Warnick, "Digital – analog magnetometer utilizing superconducting sensor," *Rev. Sci. Instrum.* vol. 38, pp. 214–220, 1967.

[2] R. P. Welty, and J. M. Martinis, "A series array of dc SQUIDs," *IEEE Trans. Magn.*, vol. 27, pp. 2924–2926, 1991.

[3] F. L. Vernon, and R. J. Pedersen, "Relaxation oscillation in Josephson juctions," *J. Appl. Phys.*, vol. 39, pp. 2661–2664, 1968.

[4] D. J. Adelerhof, H. Nijstad, J. Flokstra, and H. Rogalla, "(Double) relaxation oscillation SQUIDs with high flux-to-voltage transfer: simulations and experiments," *J. Appl. Phys.*, vol. 76, pp. 3875–3886, 1994.

[5] D. Drung, R. Cantor, M. Peters, H. J. Scheer, and H. Koch, "Low-noise high-speed dc superconducting quantum interference device magnetometer with simplified feedback electronids," *Appl. Phys. Lett.*, vol. 57, pp. 406–408, 1990.

[6] D. Drung, H. Matz, and H. Koch, "A 5 – M Hz bandwidth SQUID magnetometer with additional positive feedback," *Rev. Sci. Instrum.* vol. 66, pp. 3008–3015, 1995.

[7] M. Kiviranta, and H. Seppa, "DC-SQUID electronics based on the noise cancellation scheme," *IEEE Trans. Appl. Supercondt.*, vol. 5, pp. 2146–2148, 1995.

[8] D. Drung, "Simplified analysis of direct SQUID readout schemes," *Supercond. Sci. Technol.*, vol. 23, 065006, 2010.

[9] X. Xie *et al.*, "A voltage biased superconducting quantum interference device bootstrap circuit," *Supercond. Sci. Technol.*, vol. 23, 065016, 2010.

[10] Y. Zhang *et al.*, "Comparison of Noise Performance of the dc SQUID Bootstrap Circuit with that of the Standard Flux Modulation dc SQUID Readout Scheme," accepted by *IEEE Trans. Appl. Supercondt.*,.